Published in final edited form as:
Environ Sci Technol. 2012 November 20; 46(22): 12246–12253. doi:10.1021/es300804f.

Detection of Carbon Nanotubes in Environmental Matrices Using Programmed Thermal Analysis

Kyle Doudrick[1,*], **Pierre Herckes, Ph.D.**[2], and **Paul Westerhoff, Ph.D.**[1]

[1]Arizona State University, School of Sustainable Engineering and The Built Environment, Tempe, AZ 85287-5306

[2]Arizona State University, Department of Chemistry and Biochemistry, Tempe, AZ 85287-1604

Abstract

Carbon nanotube (CNT) production is rapidly growing, and there is a need for robust analytical methods to quantify CNTs at environmentally relevant concentrations in complex organic matrices. Because physical and thermal properties vary among different types of CNTs, we studied 14 single-walled (SWCNTs) and multiwalled CNTs (MWCNTs). Our aim was to apply a classic analytical air pollution method for separating organic (OC) and elemental carbon (EC) (thermal optical transmittance/reflectance, TOT/R) to environmental and biological matrices and CNTs. The TOT/R method required significant modification for this analysis, which required a better understanding of the thermal properties of CNTs. An evaluation of the thermal properties of CNTs revealed two classes that could be differentiated using Raman spectroscopy: thermally "weak" and "strong." Using the programmed thermal analysis (PTA) method, we optimized temperature programs and instituted a set of rules for defining the separation of OC and EC to quantify a broad range of CNTs. The combined Raman/PTA method was demonstrated using two environmentally relevant matrices (cyanobacteria (CB) and urban air). Thermal evaluation of CB revealed it to be a complex matrix with interference occurring for both weak and strong CNTs, and thus a pretreatment method was necessary. Strong CNT masses of 0.51, 2.7, and 11 μg, corresponding to concentrations of 10, 54, and 220 μg CNT/g CB, yielded recoveries of 160 ± 29%, 99 ± 1.9%, and 96 ± 3.0%, respectively. Urban air was also a complex matrix and contained a significant amount (12%) of background EC that interfered with greatly weak CNTs and minimally with strong CNTs. The current detection limit at 99% confidence for urban air samples and strong CNTs is 55 ng/m^3 (0.33 μg). Overall, the PTA method presented here provides an initial approach for quantifying a wide range of CNTs, and we identify specific future research needs to eliminate potential interferences and lower detection limits.

Keywords

carbon nanotube; multiwalled; single-walled; thermal; water; detection

INTRODUCTION

Carbon nanotube (CNT) production and usage is increasing, and consequently, concern is growing over the fate and toxicity of CNTs in the environment [1]. Multiwalled carbon nanotubes (MWCNTs) account for the majority of nanoscale carbon production. Capacity

[*]**Corresponding Author:**kdoudric@asu.edu.

Supporting information available

As referenced in article. This information is available free of charge via the Internet at http://pubs.acs.org.

estimates reached 3,400 ton/yr in 2010 with a projected increase to 9,400 ton/yr in 2015; actual production is less than 20% of capacity [2]. Large-scale production of CNTs is usually accomplished using one of two methods: electric-arc discharge (arc) or catalytic chemical vapor deposition (CVD). CVD is the most common method for large-scale production and produces yields of high purity (>90–95%), whereas the arc method is used less frequently and produces yields of lower purity (20–60%) [3]. Post-production, CNTs are usually purified, functionalized, or annealed to change their physical and chemical properties for specified applications. The production and treatment methods affect the mechanical, electrical, and thermal properties of the CNTs [3].

CNTs are challenging to quantify using traditional techniques such as mass spectrometry because of their heterogeneity in diameter, length, surface functionality, and, for single-walled CNTs (SWCNTs), chirality. Several techniques have been explored for CNT quantification (Table SI-1), including optical methods such as UV-VIS-NIR absorption [4–6], fluorescence [7, 8], and Raman spectroscopy [9]; tagging approaches such as isotopic [10, 11], fluorescence [12], and probe labeling; size-exclusion methods such as gel electrophoresis [13, 14]; and thermal analysis methods such as thermogravimetric analysis (TGA) [15, 16], temperature programmed oxidation (TPO) [17, 18], chemothermal oxidation (CTO) [19], total organic carbon (TOC) [20], and thermal optical transmittance/reflectance (TOT/R) [21–23]. These approaches have limitations, including specificity to particular CNTs or inapplicability to more complex matrices. With these current limitations and concerns over CNT fate and toxicity, there is a need to develop a strategy for CNT analysis in complex environmental matrices.

Thermal-based analytical methods are promising owing to the unique thermodynamic stability of CNTs. TGA was coupled with mass spectrometry to quantify CNTs in marine sediments using isotopic ratios of carbon in CNTs, and a detection limit of 4 μg SWCNT/40 mg sample was obtained [16]. Similarly, CTO 375°C, a soot analysis method [24], was used to quantify a range of CNTs in ultrapure water and in marine sediments [19]. Recovery values were highly dependent on the type of CNT, especially in the more complex sediment samples, and large CNT concentrations were used (25 mg CNT/g sediment). TOC was coupled successfully with an elaborate pre-oxidation method to quantify MWCNTs in rat lungs [20]; however, the chemical and thermal oxidation pretreatments used were very harsh and are known to oxidize CNTs to CO_2 [25]. TOT/R is a standard method for detecting refractory or elemental carbon (EC) (e.g., soot) in air samples [26], and it has been used to quantify MWCNTs alone [21, 22] or in a simple matrix consisting of ultrapure water and natural organic matter (NOM) [23]. Interlaboratory comparisons of organic carbon (OC)/EC separation methods (including TGA, CTO, and TOT/R) have shown that TOT/R is the most reliable technique for detecting EC in environmental matrices [27–29]. However, little evidence supports its validity for a wide range of CNTs exhibiting different thermal and physical properties. Furthermore, the thermal behavior of various environmental matrices using TOT/R is unknown, and this will be important for detecting CNTs. The CNT quantification strategy described herein is built around the TOT/R method owing to its reliability in detecting soot in air and sediment samples.

This study aims to evaluate the thermal stability of many different CNTs alone to develop a thermal analysis strategy for CNT quantification. Environmentally relevant air, water, sediment, and biological matrices were analyzed to assess potential interferences in CNT measurement from pyrolized organic matter and the presence of natural EC in water (surface and tap water, wastewater, chemical dispersants), sediments, urban air, and biological samples (urine, serum, milk, lung tissue). Our study is unique because we use 14 different CNTs produced by a range of processes that result in a span of physical and chemical properties. We discuss optimization of analysis methods for CNT detection. Demonstration

of CNT detection in two relevant environmental matrices (cyanobacteria (CB) and urban air) was completed to investigate the potential inferences on CNT quantification.

EXPERIMENTAL DETAILS

CNT Sources and Sample Preparation

CNTs (n = 14) used in this study are listed in Table 1. An array of MWCNTs were studied, including raw CVD (MW-O, MW-Mitsui, MW-15, MW-20, MW-30, MW-100), purified CVD (MW-P), functionalized CVD (MW-F, MW-OH, MW-COOH), annealed CVD (MW-15G), and raw arc (MW-Arc). Two SWCNTs were studied including a raw (SW) and purified (SW-65) CVD. Manufacturer details are provided in the Supplemental Information (SI).

CNTs were massed using a microbalance (Sartorius Micro M 500 P). CNT stock solutions were prepared by adding CNTs (10 mg/10 mL) to ultrapure water (Nanopure®, 18.3 MΩ-cm) followed by bath sonication (Branson 2510, 40 kHz) for approximately 30 minutes. Except for MW-F CNTs, Triton X-114 was added as a dispersant at a 4:1 dispersant to CNT mass ratio. X-114 had no marked effect on the thermal stability of the CNTs. Samples, ranging from 1 to 100 μL, were loaded onto pre-fired quartz fiber filters (QFF, Pallflex Tissuquartz Filters, 2500 QAT-UP). Filters were heated to 870°C prior to sample preparation to remove any carbonaceous contamination acquired during storage (e.g., dust). Aqueous samples were loaded by pipetting the desired sample volume (1–100 uL) onto the center of the filter and then allowing it to dry at approximately 90°C.

Environmental and Biological Matrices

Four dispersants (Sigma Aldrich) commonly used to create homogeneous CNT stock solutions, polydiallydimethylammonium chloride (PDDA, #409014, 20% in H_2O, average MW = 100,000–200,000 g/mol), Triton X-114 (X-114, #X-114, average MW = 537 g/mol), sodium dodecyl sulfate (SDS, #436143, >99%), and sodium deoxycholate (SDOC, #D6750, >97%) were used as received. Reservoir surface water (Saguaro Lake, DOC = 5.6 mg/L) and tap water (Tempe, AZ, DOC = 2.7 mg/L) samples were collected in July 2010. Representative wastewater samples were obtained from a laboratory activated sludge sequencing batch reactor [30]. Urban air (Arizona State University, Tempe, AZ) was collected for 24 hrs on a pre-fired QFF using a high volume air sampler. Sediments were collected from the Bread and Butter Creek, SC, an intertidal mudflat sediment containing 4.7% TC (of dry sediment mass). Biological matrices included synthetic urine (prepared as described previously [31]), human serum (Sigma Aldrich, H4522), and cow's milk (Shamrock Farms, 2%).

Extraction of CNTs from Cyanobacteria

Cyanobacteria (*Synechocystis* sp. PCC6803) were collected from a lab culture and then freeze dried. MW-Mitsui CNTs were spiked into a 50 mg sample of cyanobacteria and allowed to mix. Samples were digested with 10 mL of tetramethylammonium hydroxide (TMAH, 25% in H_2O, Sigma Aldrich 331635) at 65°C for 24 hrs, followed by centrifugation at 13,000 g. The pellet, containing non-digestible OC and CNTs, was transferred to a QFF and heat treated in air at 500°C for 15 minutes to remove low-stability organic carbon. The treated pellet was then used for further analyses.

Analytical Methods

Thermal analysis was performed using a commercial OC-EC analyzer equipped with optical correction (Sunset Laboratory, Inc., Forest Grove, OR). The instrument is commonly used for NIOSH soot determinations as well as atmospheric OC and EC measurements in air

pollution studies. Instrument details are provided in the SI, and a schematic of the instrument setup is shown in Figure SI-1.

The EC-OC instrument is controlled through user-defined temperature programs, which emerged as critical for CNT analysis. These programs allow the temperature, temperature residence time, and carrier gas to be adjusted according to the type of sample under analysis. Although this instrument is standard for analysis of air pollutants, its operation is briefly described because optimization for CNT analysis requires a basic understanding. For this study, an inert (100% He) and an oxidizing carrier gas (90%He/10% O_2) were used with temperatures ranging from 0 to 910°C. Samples were first heated under inert conditions to remove volatile OC. The sample chamber was then cooled and switched to oxidizing conditions. OC that does not volatilize may undergo pyrolysis becoming pyrolytically generated elemental carbon (PEC; i.e., char), which has thermal properties similar to EC. Fixed or variable residence times can be used at each temperature step, where variable residence times are defined by a minimum and maximum time that allows for complete desorption at each temperature step. Variable residence times were used during the inert phase to allow for complete desorption of OC so as to minimize interferences with EC during the oxidizing phase. Both variable and fixed residence times were used during the oxidizing phase and depended on the sample matrix and CNT type.

As the sample is analyzed, the volatilized and combusted carbon travels to an oxidizing oven (MnO_2 catalyst at 870°C), where it is transformed into carbon dioxide (CO_2). The CO_2 passes through a methanator (Ni firebrick–supported catalyst) and is reduced to methane (CH_4). The CH_4 signal is measured using a flame ionization detector (FID) and is converted to TC using a CH_4 standard. TC is split into two types of carbon post-analysis: OC and EC. The portion of TC that is OC or EC is defined by the method, which determines where the OC-EC split is placed post-analysis. This split can be automatic on the basis of automatic optical correction; the optical transmittance or reflectance is observed throughout analysis using a 632 nm laser, and the split is placed where the transmittance/reflectance returns to the initial reading. For samples in which optical correction does not work, a manual split defined by the analyst should be used. For samples containing no PEC, the split can be placed between the two carrier gas modes; everything to the left of the split (inert conditions) would be OC, and everything to the right (oxidizing conditions) would be EC. This method is based on the assumption that EC is stable under inert conditions and that OC is not. If PEC is present but combusts at lower temperatures than the EC under analysis, then a manual split can be placed between OC and EC, usually at a defined temperature. If the PEC overlaps with the EC, then the manual split must be placed where interference is minimal. Figure SI-2 shows a sample thermogram of sucrose using the NIOSH temperature program [26, 32] and how OC, EC, and PEC are traditionally defined using optical correction.

The automatic optical correction (i.e., TOT/R) is successful when using well dispersed CNTs that can be loaded homogeneously on the filter at concentrations that allow for proper transmittance [23]. However, optical correction will err when dealing with CNT samples that are more indicative of that found in the environment (e.g., aggregated, low concentrations), such that only a few aggregates are heterogeneously dispersed on the filter [28, 29]. For all CNTs examined (Table 1), the optical correction method was not reliable, and a manual split method was required for aqueous and solid samples (see the SI for further discussion). Because of the lack of optical correction, the thermal analysis method discussed herein for CNTs is referred to as programmed thermal analysis (PTA).

Raman spectroscopy was performed on a custom-built instrument in 180° geometry. The sample was excited using a 532-nm laser with 100-mW maximum power, which was

controlled using neutral density filters. The data were collected using an Acton 300i spectrograph and a back thinned Princeton Instruments liquid nitrogen cooled CCD detector with a spatial resolution <1 μm and spectral resolution of <1 cm^{-1}.

For analysis of the CNTs, dry powders were loaded onto quartz slides, and spectral analysis was done in triplicate. Analysis of CNTs in environmental matrices was performed directly on the QFF. For all samples, the background was subtracted from the spectra.

RESULTS AND DISCUSSION

CNT Thermal Stability and Method Optimization

Using the manual split method to quantify CNTs in complex matrices requires a deeper understanding of the thermal behavior of CNTs under both inert and oxidizing conditions. This method cannot be developed around one type of CNT because CNTs have different thermal properties depending on whether they are single-walled, multiwalled, functionalized, annealed, etc. To optimize a set of temperature programs for a range of CNTs, we first analyzed a representative group of CNTs (Table 1) under inert conditions to determine the maximum temperature at which no CNT loss occurs, and then analyzed them under oxidizing conditions to determine the minimum temperature at which the CNTs begin to combust.

Figure 1 shows the fraction of CNT mass remaining after heating to 870°C under inert conditions for several CNTs. This is the maximum temperature used in the NIOSH program and previous CNT thermal studies [21, 23, 26]. Mass loss curves for this and subsequent figures were generated by integrating the thermogram FID signal (e.g., Figure SI-4). In Figure 1, the raw CVD MWCNTs (MW-O, MW-15, MW-20, MW-30, MW-100) were represented by MW-O and MW-15, the functionalized MWCNTs (MW-F, MW-OH, MW-COOH) by MW-F, the purified MWCNTs by MW-P, the graphitized or ordered MWCNTs (MW-Arc, MW-15G, MW-Mitsui) by MW-Arc, and the SWCNTs (SW, SW-65) by SW-65. Figure 1 shows that only the graphitized MWCNTs were stable under inert conditions up to 870°C. The MW-P CNTs were the least stable, exhibiting nearly 100% mass loss after ~1000 seconds at 870°C. All CVD MWCNTs were unstable at 870°C, and they exhibited mass loss with what appears to be a zero-order rate. Thus, using the temperature programs outlined in existing methods is not valid for all CNTs.

Several factors could have influenced the observed range of CNT thermal stability including functional group content, metal catalyst content, and defect density. If oxygenated groups were responsible for the observed mass loss (Figure 1) then the expected order of mass loss rate should follow MW-O ~ MW-P < MW-F; however, the rate of mass loss followed MW-P < MW-O < MW-F. The MW-O had the most metal (oxide) impurities (4.49% Ni/0.76% Fe), but they were more stable than MW-P (1.80% Ni/0.08% Fe). Furthermore, the MW-Mitsui CNTs, which contained ~10% iron impurities, did not exhibit any mass loss. This suggests that, for MWCNTs, oxygen associated with functional groups or metals does not affect the rate of mass loss under inert conditions. The difference in thermal stabilities between CNTs under inert conditions may be explained by the defect density rather than the abundance of oxygenated functional groups or metal oxides. MWCNTs produced by CVD will generate additional defects when heated under inert conditions until a limiting temperature is reached, at which point the defects begin to heal [33]. If this temperature is not reached, then defects may continue to develop. High-temperature annealing of CNTs reorders the sp^3 bonds to sp^2, which makes them more thermally stable [34–39]. For CNTs created or treated at high temperatures (>2500°C), such as MW-Arc and MW-15G, respectively, no defects were introduced because they had already reached a high state of thermodynamic stability. Also, no mass loss was observed for MW-15G, unlike MW-15; the

only difference between the two was thermal treatment. Although defects are likely the cause of mass loss under inert conditions, the mechanisms behind this are unknown. Sublimation has been shown to occur for C_{60} under inert heating conditions [40], but similar behavior has yet to be shown to occur for CNTs.

To optimize the temperature program for the CNTs exhibiting mass loss under inert conditions, the MW-O, MW-P, MW-F, and SG-65 CNTs were analyzed at several maximum temperatures, including 675, 700, 750, and 870°C (MW-O shown in Figure SI-5). No significant (<5%) CNT mass loss occurred below 675°C for any CNTs in this study. The minimal CNT mass loss (<5%) observed at temperatures as low as ~250°C was attributed to either oxidation caused by oxygen associated with surface C atoms or amorphous carbon (Figure SI-4).

The thermal behavior of CNTs was examined under oxidizing conditions to determine the temperature at which CNTs begin to combust as well as the maximum temperature required to completely oxidize the CNTs. Figure 2 shows the fraction of CNT mass remaining with increasing temperature under oxidizing conditions. MW-F and MW-O CNTs were representative of all other MWCNTs not shown in Figure 2 (all mass loss curves are shown in Figure SI-6). The purified SWCNTs (SW-65) were the least stable CNTs, with almost 100% mass loss occurring before 650°C. Most of the weak CNTs began combusting at ~650°C and reached a maximum rate at ~700°C. MW-15 also started combustion between 650 and 700°C, but at a slower rate than other weak CNTs, which suggests that MW-15 represents the upper limit of the weak CNTs. Similar to inert conditions, under oxidizing conditions MW-Arc, MW-Mitsui, and MW-15G were more stable than all other CNTs; their initial oxidation temperatures ranged from ~750 to 800°C. When a weak CNT (MW-15) was annealed at ~2000°C (MW-15G), the rate of mass loss was decreased. The MW-Arc CNTs, which are synthesized at greater than 3000°C, were the most stable; most of their oxidation occurred above 900°C. This is consistent with previous studies that showed MWCNTs produced by arc were much more stable than those produced using CVD [41, 42]. No linear correlation was found between thermal stability and CNT diameter, unlike as shown previously for CNTs synthesized by a common method [38], which in our case may be attributed to the differences in CNT production temperature rather than diameter.

On the basis of these results, the CNTs can be grouped into two thermal classifications: CNTs that are stable at the maximum temperature (870°C) under inert conditions and did not begin oxidation until ~750–800°C were classified as thermally “strong,” and CNTs that are not stable above ~700°C under inert conditions were classified as thermally “weak.” The range of weak CNTs was much broader; the SG-65 and MW-15 represent the lower and upper bounds, respectively. Whereas MWCNTs are classified by their defect density, SWCNTs are classified as weak because of their small diameter and high percentage (~100%) of surface atoms, which decreases thermal stability due to an increase in bond strain [43] and a larger number of carbon atoms exposed to oxygen, respectively.

“Weak” and “Strong” Classification Using Raman Spectroscopy

Raman spectroscopy has been shown to be a reliable characterization tool for CNTs with spectral peaks that are specific to graphitic carbon [44]. Between 1300 and 1600 cm^{-1}, there are two distinct peaks for CNTs, called the D-band (~1350 cm^{-1}) and the G-band (~1580 cm^{-1}) (Figure SI-7a). The D-band indicates disorder present within the CNT sample, and its intensity is proportional to defect density. The G-band is a result of C-C bond stretching unique to sp^2 hybridizations found in graphitic carbon. The ratio of the D-band and G-band intensities (I_D/I_G) is often used to quantify the defectiveness of CNTs, and this ratio can be used to estimate the thermal stability of CNTs [33, 36, 38, 42, 45, 46]. Another advantage of Raman spectroscopy is that it can be used to distinguish between SWCNTs and MWCNTs

by inspection of the radial breathing mode (RBM) at lower frequencies [44]. For SWCNTs, there will be multiple peaks between 100 and 300 cm^{-1}, whereas MWCNTs will have no characteristic peaks (Figure SI-7b). If RBM peaks are present, then the sample will be classified as weak, independent of the I_D/I_G ratio.

Raman spectroscopy was used to distinguish thermally "strong" from "weak" CNTs. There is a strong linear relationship ($R^2 = 0.96$) between the I_D/I_G ratio and the temperature at 50% CNT mass loss (Figure 3, Table SI-2). MWCNTs with $I_D/I_G > 0.60$ and SWCNTs were synonymous with weak CNTs, and MWCNTs with $I_D/I_G \leq 0.60$ with strong CNTs. This suggests that Raman spectroscopy can be used to determine the thermal stability classification of the CNT (i.e., weak or strong), which can then be used to determine the approximate temperature at which the CNTs will combust. The key to using Raman for CNT thermal classification will be to eliminate background Raman peaks by extracting the CNTs from the sample. If the CNT type cannot be determined using Raman spectroscopy, then assuming the CNTs to be weak would be an appropriate conservative estimate.

Thermal Behavior of Environmental and Biological Matrices

Under inert conditions organic matter can form PEC, and this may cause interference if it combusts in the same temperature range as CNTs. Furthermore, environmental samples that have been exposed to anthropogenic EC such as wastewater sludge, air, soils, and sediments can also cause interference. We define all "non-CNT EC" evolving during the oxidizing phase as NEC, and this includes PEC, anthropogenic EC (e.g., soot), and natural EC.

Figure 4a shows the percent NEC (μg NEC/μg TC × 100%) generated under inert conditions for several environmental and biological matrices. The NEC percentage was independent of the TC loading and used to quantify charring of organic matter and the presence of background EC. The dispersants, which are free of background EC, had negligible NEC (<1%), which indicates little PEC formation. Of the environmental matrices, surface water and lab activated sludge had less than 10% NEC, and the urban air and sediment samples had a substantial amount of NEC, which is most likely attributed to the background EC (e.g., soot). Of the biological matrices, urine had very little NEC, whereas lung tissue, milk, and human serum had high NEC percentages, most likely owing to charring of fats and proteins rather than background EC. Matrices that had less than 10% NEC content were defined as "simple," and those that that had greater than 10% NEC were defined as "complex."

Figure 4b shows the percent NEC mass remaining for complex matrices and percent EC mass remaining for three CNTs with increasing temperature under oxidizing conditions. MW-F and MW-15 CNTs represent the average and upper bound of the thermally weak CNTs, respectively, and MW-Arc represents the thermally strong CNTs. Of the environmental and biological samples examined, the simple matrices had less than 5% interference at combustion temperature ranges similar to both the weak and strong CNTs, whereas the complex matrices had more substantial interferences depending on the CNT classification. All of the complex matrices were observed to overlap with all weak CNTs to some degree. The most substantial interference with weak CNTs was observed for the sediment and urban air samples, which may be due to thermally stable EC (e.g., soot). The biological samples exhibited <5% interference with the upper bound weak CNTs (MW-15), but approximately 10% and 20% of the urban air and sediment samples, respectively, remained when the MW-15 CNTs began oxidizing. No matrices exhibited any significant (>5%) interference with the strong CNTs. On the basis of these results, complex matrices will interfere with weak CNTs during the oxidizing phase (Figure 2). Furthermore, these complex matrices have OC that desorbs at the same temperature as the weak CNTs under inert conditions (Figure 1); this makes interference even more significant, especially if long residence times at temperatures greater than 700°C are required to remove the OC.

Given the small sample size of the matrices tested, even the smallest amount of interference can compound in a larger environmental sample to overshadow the CNT signal. For example, 5.0 μL of human serum contained 200 μg of TC, of which 26 μg was considered NEC and 15 μg (7.5%) and 0.16 μg (0.08%) interfered with weak and strong CNTs, respectively. A procedure was developed to account for these potential interferences. First, an optimized temperature program for thermally strong and weak CNTs, differentiated using Raman spectroscopy, must be used. Second, digestion techniques must be used to degrade organic matter to prevent PEC formation (see below). However, the digestion technique should be non-selective for CNTs such that they will not be degraded to CO_2, as is observed with harsh chemical oxidant digestion methods. Techniques to separate graphitic EC from CNTs in soils, sediments, sludge, and air will be more challenging to develop because of their similar chemical and thermal properties

Demonstration of CNT Detection in Environmental Matrices

We have outlined a method that can be used to identify the thermal classification of CNTs using Raman spectroscopy followed by quantification using PTA. Using two different environmental matrices, cyanobacteria and urban air, the applicability of this method is demonstrated for a strong CNT (MW-Mitsui). Weak CNTs require development of more elaborate extraction methods that are beyond the scope of this study. CB were selected because they are a ubiquitous primary producer in surface waters, and research has suggested that they may be a good indicator organism for ecotoxicity tests [47, 48]. Similarly, green algae have been used as an indicator organism to examine the toxicity effects of CNTs [49–52].

CB (50 mg dry-weight) was spiked with 0.51, 2.7, and 11 μg of MW-Mitsui MWCNTs corresponding to a mass ratio of 10, 54, and 220 μg CNTs/g CB, respectively. Recovery is expressed as the mean and standard error of triplicate samples. After pre-treatment, samples were loaded onto a QFF and then analyzed with Raman spectroscopy. CNT aggregates were easily located using the Raman microscope due to their opacity, and a spectrum with clear CNT peaks was obtained with relatively low noise (Figure SI-8). The important steps for isolating CNT aggregates for Raman spectroscopy were: (1) extracting the CNTs by digesting the CB and (2) centrifuging the sample to aggregate the CNTs. The I_D/I_G ratio was 0.26 ± 0.08, which would appropriately classify the CNTs as “strong.” After Raman analysis, the samples were analyzed using PTA with an OC/EC split point at 750°C. CNT mass recovery for 10 μg CNTs/g CB, 54 μg CNTs/g CB, and 220 μg CNTs/g CB was 160 ± 29%, 99 ± 1.9%, and 96 ± 3.0%, respectively. Although CB is a relatively simple matrix (i.e., no background EC), a small amount (~0.20 μg) of interference is still caused by PEC formation, which evolves at the same temperature as the MW-Mitsui CNTs. Although the interference had little effect on larger CNT masses (e.g., 2.7 and 11 μg) and excellent recoveries were obtained, it was significant enough that when the CNT mass was closer to the interference mass, the recovery was less accurate. PTA is appropriate for exposure studies using CB as an indicator organism, but dosage levels should be greater than 10 μg CNTs/g CB (dry) to obtain reliable recoveries.

Graphitic particles are ubiquitous in soils, sediments, air, and wastewater sludge, and these will have a thermal stability very close to if not greater than CNTs. Urban air contains EC that combusts at the same temperature as the weak CNTs (i.e., Figure 4b), thus making it difficult to detect a low concentration of CNTs in an urban air sample with a large EC content (Figure SI-9a). However, less interference occurs with the strong CNTs (Figure SI-9b). Urban air samples (1.5 cm^2 filter punch) were spiked with 2.8 μg (465 ng/m^3) of MW-Mitsui CNTs and analyzed using PTA. Recovery is expressed as the mean and standard error of nine replicates. The CNTs began combusting at ~750°C, which was used to develop the temperature program and the location of the split point. A non-spiked urban air

sample from the same filter contained 45 μg (7,477 ng/m^3) of TC, with 12% (5.5 μg, 914 ng/m^3) EC as determined by optical correction, and 0.46% (0.21 μg, 35 ng/m^3) combusting after 750°C. The mean mass of nine replicates was 2.8 μg with a standard deviation of 0.11 μg resulting in a recovery of 100 ± 4.0%. The EPA standard method was used to calculate detection limits [53]. The method detection limit (MDL) with 99% confidence was calculated to be 55 ng/m^3 (0.33 μg). The lower critical limit (LCL) and the upper critical limit (UCL) for 95% confidence were calculated to be 22 ng/m^3 (0.13 μg) and 76 ng/m^3 (0.46 μg), respectively. The limit of detection (LOD) and limit of quantitation (LOQ) were calculated to be approximately 136 ng/m^3 (0.82 μg) and 183 ng/m^3 (1.1 μg), respectively.

Applicability and Future Development Needs

A temperature program specific to different CNTs and environmental matrices is required for reliable quantification. CNTs have a wide range of initial oxidation temperatures ranging from approximately 500°C to 800°C; most initial oxidation occurs at ~650°C. The temperature programs will depend on the matrix under analysis and the split point on the type of CNT. For weak CNTs, the maximum temperature that should be used during inert conditions is 675°C, and if higher temperatures are required, then small residence times should be employed to reduce CNT mass loss. During oxidizing conditions, the highest temperature should be a minimum of 800°C to ensure complete CNT oxidation.

Currently, the method described herein is ideal for working at concentrations commonly used in toxicity studies [1, 54–57] for strong CNTs and some weak CNTs in controlled experiments (e.g., toxicity tests, lab-scale removal tests). The future challenge will be processing large volumes of CNT-containing sample (e.g., wastewater) or CNTs in samples containing large amounts of interfering carbon (e.g., soils). Extraction, separation, and purification steps are key to working with such samples. Our work with TMAH represents the first step in such a pre-treatment strategy, but additional work is needed on the Raman/PTA approach demonstrated here before it can be applied to environmental monitoring at trace levels.

Supplementary Material

Refer to Web version on PubMed Central for supplementary material.

Acknowledgments

This work was supported by the NIH Grand Opportunities (RC2) program through NANO-GO NIEHS grant DE-FG02-08ER64613. Instruments used for material characterization were provided by the ASU LeRoy Eyring Center for Solid State Science. We greatly appreciate Dr. Matt Fraser for providing access to the OC/EC instrument and Andrea Clements for her expert knowledge and assistance with the instrument. We thank the following people for donating materials: Dr. Som Mitra, New Jersey Institute of Technology, for providing the MW-O, -P, and -F MWCNTs; Dr. Günter Oberdörster, The University of Rochester, for the Mitsui MWCNTs; and Dr. Ariette Schierz, Duke University, for the SG-65 SWCNTs and Bread and Butter Creek sediment samples.

REFERENCES

1. Lam CW, James JT, McCluskey R, Arepalli S, Hunter RL. A review of carbon nanotube toxicity and assessment of potential occupational and environmental health risks. Crit. Rev. Toxicol. 2006; 36(3):189–217. [PubMed: 16686422]
2. Innovative Research and Products, Inc. Production and applications of carbon nanotubes, carbon nanofibers, fullerenes, graphene, and nanodiamonds: A global technology survey and market analysis. 2011:531. ET-113.
3. Carbon Nanotubes: Science and Applications. Boca Raton, FL: CRC Press LLC; 2005.

4. Bahr JL, Mickelson ET, Bronikowski MJ, Smalley RE, Tour JM. Dissolution of small diameter single-wall carbon nanotubes in organic solvents? Chem. Commun. 2001; (2):193–194.
5. Li ZF, Luo GH, Zhou WP, Wei F, Xiang R, Liu YP. The quantitative characterization of the concentration and dispersion of multi-walled carbon nanotubes in suspension by spectrophotometry. Nanotechnology. 2006; 17(15):3692–3698.
6. Jeong SH, Kim KK, Jeong SJ, An KH, Lee SH, Lee YH. Optical absorption spectroscopy for determining carbon nanotube concentration in solution. Synth. Met. 2007; 157(13–15):570–574.
7. O'Connell MJ, Bachilo SM, Huffman CB, Moore VC, Strano MS, Haroz EH, Rialon KL, Boul PJ, Noon WH, Kittrell C, Ma JP, Hauge RH, Weisman RB, Smalley RE. Band gap fluorescence from individual single-walled carbon nanotubes. Science. 2002; 297(5581):593–596. [PubMed: 12142535]
8. Huang H, Zou M, Xu X, Liu F, Li N, Wang X. Near-infrared fluorescence spectroscopy of single-walled carbon nanotubes and its applications. TrAC-Trends Anal. Chem. 2011; 30(7):1109–1119.
9. Salzmann CG, Chu BTT, Tobias G, Llewellyn SA, Green MLH. Quantitative assessment of carbon nanotube dispersions by Raman spectroscopy. Carbon. 2007; 45(5):907–912.
10. Petersen EJ, Huang QG, Weber WJ. Bioaccumulation of radio-labeled carbon nanotubes by Eisenia foetida. Environ. Sci. Technol. 2008; 42(8):3090–3095. [PubMed: 18497171]
11. Zhang LW, Petersen EJ, Huang QG. Phase Distribution of C-14-Labeled Multiwalled Carbon Nanotubes in Aqueous Systems Containing Model Solids: Peat. Environ. Sci. Technol. 2011; 45(4):1356–1362. [PubMed: 21222444]
12. Xiao H, Zou HF, Pan CS, Jiang XG, Le XC, Yang L. Quantitative determination of oxidized carbon nanotube probes in yeast by capillary electrophoresis with laser-induced fluorescence detection. Anal. Chim. Acta. 2006; 580(2):194–199. [PubMed: 17723773]
13. Wang RH, Mikoryak C, Chen E, Li S, Pantano P, Draper RK. Gel Electrophoresis Method to Measure the Concentration of Single-Walled Carbon Nanotubes Extracted from Biological Tissue. Anal. Chem. 2009; 81(8):2944–2952. [PubMed: 19296592]
14. Wang RH, Mikoryak C, Li SY, Bushdiecker D, Musselman IH, Pantano P, Draper RK. Cytotoxicity Screening of Single-Walled Carbon Nanotubes: Detection and Removal of Cytotoxic Contaminants from Carboxylated Carbon Nanotubes. Mol. Pharm. 2011; 8(4):1351–1361. [PubMed: 21688794]
15. Pang LSK, Saxby JD, Chatfield SP. Thermogravimetric analysis of carbon nanotubes and nanoparticles. J. Phys. Chem. 1993; 97(27):6941–6942.
16. Plata DL, Reddy CM, Gschwend PM. Thermogravimetry-mass spectrometry for carbon nanotube detection in complex mixtures. Environ. Sci. Technol. 2012 *(In press)*.
17. Alvarez WE, Kitiyanan B, Borgna A, Resasco DE. Synergism of Co and Mo in the catalytic production of single-wall carbon nanotubes by decomposition of CO. Carbon. 2001; 39(4):547–558.
18. Herrera JE, Resasco DE. In situ TPO/Raman to characterize single-walled carbon nanotubes. Chem. Phys. Lett. 2003; 376(3–4):302–309.
19. Sobek A, Bucheli TD. Testing the resistance of single- and multi-walled carbon nanotubes to chemothermal oxidation used to isolate soots from environmental samples. Environ. Poll. 2009; 157(4):1065–1071.
20. Tamura M, Inada M, Nakazato T, Yamamoto K, Endo S, Uchida K, Horie M, Fukui H, Iwahashi H, Kobayashi N, Morimoto Y, Tao H. A determination method of pristine multiwall carbon nanotubes in rat lungs after intratracheal instillation exposure by combustive oxidation-nondispersive infrared analysis. Talanta. 2011; 84(3):802–808. [PubMed: 21482285]
21. Myojo T, Oyabu T, Nishi K, Kadoya C, Tanaka I, Ono-Ogasawara M, Sakae H, Shirai T. Aerosol generation and measurement of multi-wall carbon nanotubes. J. Nanopart. Res. 2009; 11(1):91–99.
22. Ono-Ogasawara M, Serita F, Takaya M. Distinguishing nanomaterial particles from background airborne particulate matter for quantitative exposure assessment. J. Nanopart. Res. 2009; 11(7): 1651–1659.
23. Hyung H, Fortner JD, Hughes JB, Kim JH. Natural organic matter stabilizes carbon nanotubes in the aqueous phase. Environ. Sci. Technol. 2007; 41(1):179–184. [PubMed: 17265945]

24. Gustafsson O, Bucheli TD, Kukulska Z, Andersson M, Largeau C, Rouzaud JN, Reddy CM, Eglinton TI. Evaluation of a protocol for the quantification of black carbon in sediments. Global Biogeochem. Cycles. 2001; 15(4):881–890.
25. Rosca ID, Watari F, Uo M, Akaska T. Oxidation of multiwalled carbon nanotubes by nitric acid. Carbon. 2005; 43(15):3124–3131.
26. National Institute for Occupational Safety and Health, Elemental Carbon (Diesel Particulate): Method 5040. NIOSH Manual of Analytical Methods, 4th Edition. 2003.
27. Watson JG, Chow JC, Chen L-WA. Summary of Organic and Elemental Carbon/Black Carbon Analysis Methods and Intercomparisons. Aerosol Air Qual. Res. 2005; 5(1):65–102.
28. Schmid H, Laskus L, Abraham HJ, Baltensperger U, Lavanchy V, Bizjak M, Burba P, Cachier H, Crow D, Chow J, Gnauk T, Even A, ten Brink HM, Giesen KP, Hitzenberger R, Hueglin C, Maenhaut W, Pio C, Carvalho A, Putaud JP, Toom-Sauntry D, Puxbaum H. Results of the "carbon conference" international aerosol carbon round robin test stage I. Atmos. Environ. 2001; 35(12): 2111–2121.
29. Hammes K, Schmidt MWI, Smernik RJ, Currie LA, Ball WP, Nguyen TH, Louchouarn P, Houel S, Gustafsson O, Elmquist M, Cornelissen G, Skjemstad JO, Masiello CA, Song J, Peng P, Mitra S, Dunn JC, Hatcher PG, Hockaday WC, Smith DM, Hartkopf-Froeder C, Boehmer A, Luer B, Huebert BJ, Amelung W, Brodowski S, Huang L, Zhang W, Gschwend PM, Flores-Cervantes DX, Largeau C, Rouzaud JN, Rumpel C, Guggenberger G, Kaiser K, Rodionov A, Gonzalez-Vila FJ, Gonzalez-Perez JA, de la Rosa JM, Manning DAC, Lopez-Capel E, Ding L. Comparison of quantification methods to measure fire-derived (black/elemental) carbon in soils and sediments using reference materials from soil, water, sediment and the atmosphere. Global Biogeochem. Cycles. 2007; 21(3):18.
30. Wang Y, Westerhoff P, Hristovski K. Fate and biological effects of silver, titanium dioxide, and C_{60} (fullerene) nanomaterials during simulated wastewater treatment processes. J. Haz. Mater. 2011 *(In-press)*.
31. Wenzler-Rottele S, Dettenkofer M, Schmidt-Eisenlohr E, Gregersen A, Schulte-Monting J, Tvede M. Comparison in a laboratory model between the performance of a urinary closed system bag with double non-return valve and that of a single valve system. Infection. 2006; 34(4):214–218. [PubMed: 16896580]
32. Birch ME, Cary RA. Elemental carbon-based method for monitoring occupational exposures to particulate diesel exhaust. Aerosol Sci. Technol. 1996; 25(3):221–241.
33. Bhalerao GM, Sinha AK, Sathe V. Defect-dependent annealing behavior of multi-walled carbon nanotubes. Physica E Low Dimens. Syst. Nanostruct. 2008; 41(1):54–59.
34. Andrews R, Jacques D, Qian D, Dickey EC. Purification and structural annealing of multiwalled carbon nanotubes at graphitization temperatures. Carbon. 2001; 39(11):1681–1687.
35. Bom D, Andrews R, Jacques D, Anthony J, Chen BL, Meier MS, Selegue JP. Thermogravimetric analysis of the oxidation of multiwalled carbon nanotubes: Evidence for the role of defect sites in carbon nanotube chemistry. Nano Lett. 2002; 2(6):615–619.
36. Kim YA, Hayashi T, Osawa K, Dresselhaus MS, Endo M. Annealing effect on disordered multi-wall carbon nanotubes. Chem. Phys. Lett. 2003; 380(3–4):319–324.
37. Ray SC, Pao CW, Tsai HM, Chen HC, Chen YS, Wu SL, Ling DC, Lin IN, Pong WF, Gupta S, Giorcelli M, Bianco S, Musso S, Tagliaferro A. High-Temperature Annealing Effects on Multiwalled Carbon Nanotubes: Electronic Structure, Field Emission and Magnetic Behaviors. J. Nanosci. Nanotechnol. 2009; 9(12):6799–6805. [PubMed: 19908682]
38. Singh DK, Iyer PK, Giri PK. Diameter dependence of oxidative stability in multiwalled carbon nanotubes: Role of defects and effect of vacuum annealing. J. Appl. Phys. 2010; 108(8):10.
39. Zhang H, Sun CH, Li F, Li HX, Cheng HM. Purification of multiwalled carbon nanotubes by annealing and extraction based on the difference in van der Waals potential. J. Phys. Chem. B. 2006; 110(19):9477–9481. [PubMed: 16686493]
40. Milliken J, Keller TM, Baronavski AP, McElvany SW, Callahan JH, Nelson HH. Thermal and oxidative analyses of buckminsterfullerene, C_{60}. Chem. Mater. 1991; 3(3):386–387.
41. Watts PCP, Hsu WK, Kroto HW, Walton DRM. Are bulk defective carbon nanotubes less electrically conducting? Nano Lett. 2003; 3(4):549–553.

42. Behler K, Osswald S, Ye H, Dimovski S, Gogotsi Y. Effect of thermal treatment on the structure of multi-walled carbon nanotubes. J. Nanopart. Res. 2006; 8(5):615–625.
43. Yao N, Lordi V, Ma SXC, Dujardin E, Krishnan A, Treacy MMJ, Ebbesen TW. Structure and oxidation patterns of carbon nanotubes. J. Mater. Res. 1998; 13(9):2432–2437.
44. Dresselhaus MS, Dresselhaus G, Saito R, Jorio A. Raman spectroscopy of carbon nanotubes. Phys. Rep. 2005; 409(2):47–99.
45. Chen J, Shan JY, Tsukada T, Munekane F, Kuno A, Matsuo M, Hayashi T, Kim YA, Endo M. The structural evolution of thin multi-walled carbon nanotubes during isothermal annealing. Carbon. 2007; 45(2):274–280.
46. Tran MQ, Tridech C, Alfrey A, Bismarck A, Shaffer MSP. Thermal oxidative cutting of multi-walled carbon nanotubes. Carbon. 2007; 45(12):2341–2350.
47. Ando T, Nagase H, Eguchi K, Hirooka T, Nakamura T, Miyamoto K, Hirata K. A novel method using cyanobacteria for ecotoxicity test of veterinary antimicrobial agents. Environ. Toxicol. Chem. 2007; 26(4):601–606. [PubMed: 17447543]
48. Aslim B, Ozturk S. Toxicity of herbicides to cyanobacterial isolates. J. Environ. Biol. 2009; 30(3): 381–384. [PubMed: 20120462]
49. Blaise C, Gagne F, Ferard JF, Eullaffroy P. Ecotoxicity of selected nano-materials to aquatic organisms. Environ. Toxicol. 2008; 23(5):591–598. [PubMed: 18528913]
50. Wei LP, Thakkar M, Chen YH, Ntim SA, Mitra S, Zhang XY. Cytotoxicity effects of water dispersible oxidized multiwalled carbon nanotubes on marine alga, Dunaliella tertiolecta. Aquat. Toxicol. 2010; 100(2):194–201. [PubMed: 20673592]
51. Basiuk EV, Ochoa-Olmos OE, De la Mora-Estrada LF. Ecotoxicological Effects of Carbon Nanomaterials on Algae, Fungi and Plants. J. Nanosci. Nanotechnol. 2011; 11(4):3016–3038. [PubMed: 21776669]
52. Schwab F, Bucheli TD, Lukhele LP, Magrez A, Nowack B, Sigg L, Knauer K. Are Carbon Nanotube Effects on Green Algae Caused by Shading and Agglomeration? Environ. Sci. Technol. 2011; 45(14):6136–6144. [PubMed: 21702508]
53. EPA, U.S. PART 136—Guidelines establishing test procedures for the analysis of pollutants. Definition and Procedure for the Determination of the Method Detection Limit—Revision 1.11. In Vol. Federal Register, 49 FR 43430 (10/26/84), 50 FR 694 (1/4/85), and 51 FR (6/30/86).
54. Petersen EJ, Akkanen J, Kukkonen JVK, Weber WJ. Biological Uptake and Depuration of Carbon Nanotubes by *Daphnia magna*. Environ. Sci. Technol. 2009; 43(8):2969–2975. [PubMed: 19475979]
55. Uo M, Akasaka T, Watari F, Sato Y, Tohji K. Toxicity evaluations of various carbon nanomaterials. Dent. Mater. 2011; 30(3):245–263.
56. Zhao XC, Liu RT. Recent progress and perspectives on the toxicity of carbon nanotubes at organism, organ, cell, and biomacromolecule levels. Environ. Int. 2012; 40:244–255. [PubMed: 22244841]
57. Firme CP, Bandaru PR. Toxicity issues in the application of carbon nanotubes to biological systems. Nanomed.-Nanotechnol. 2010; 6(2):245–256.

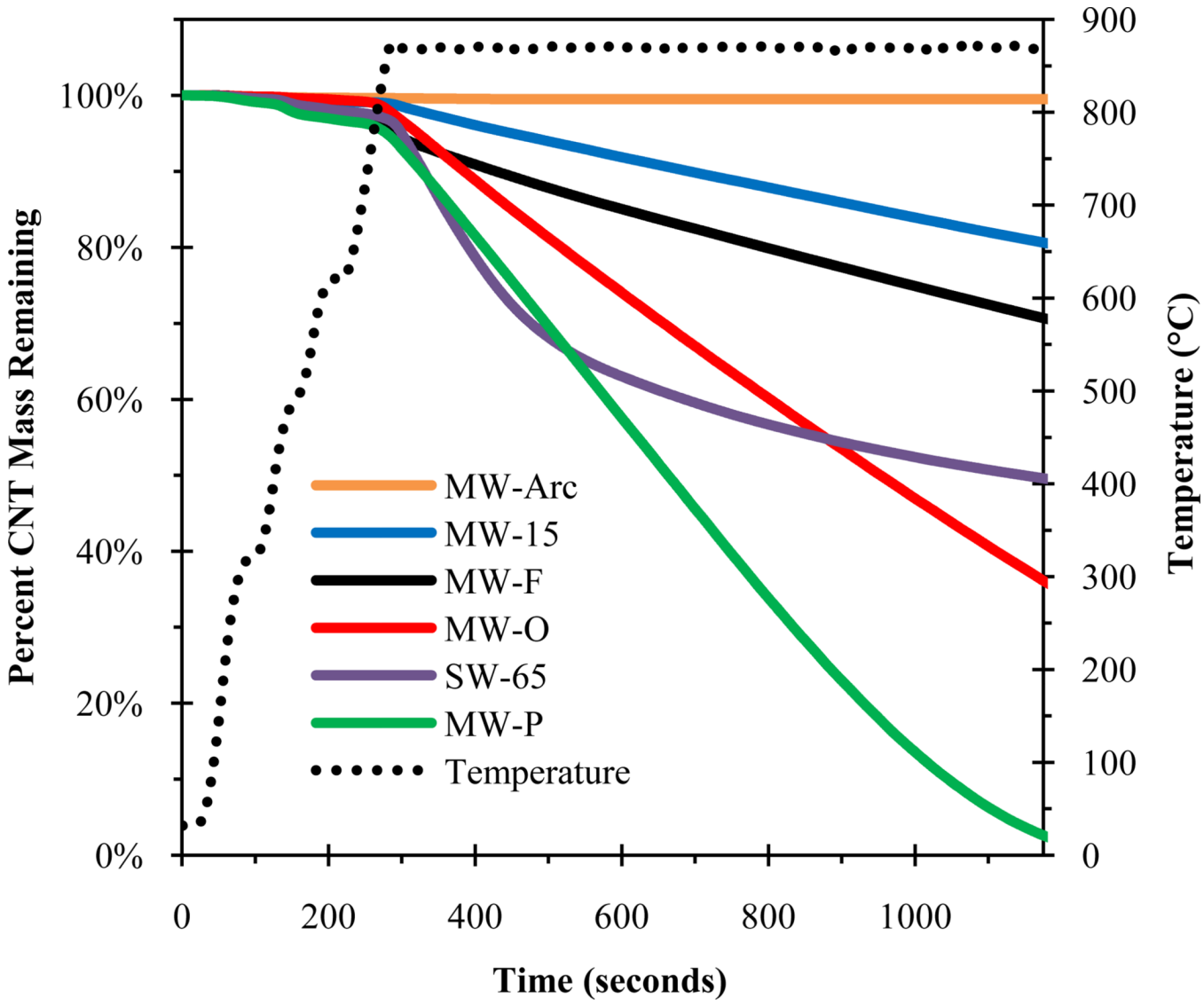

Figure 1.
Percent CNT mass remaining after heating to 870°C under inert conditions for several CNTs.

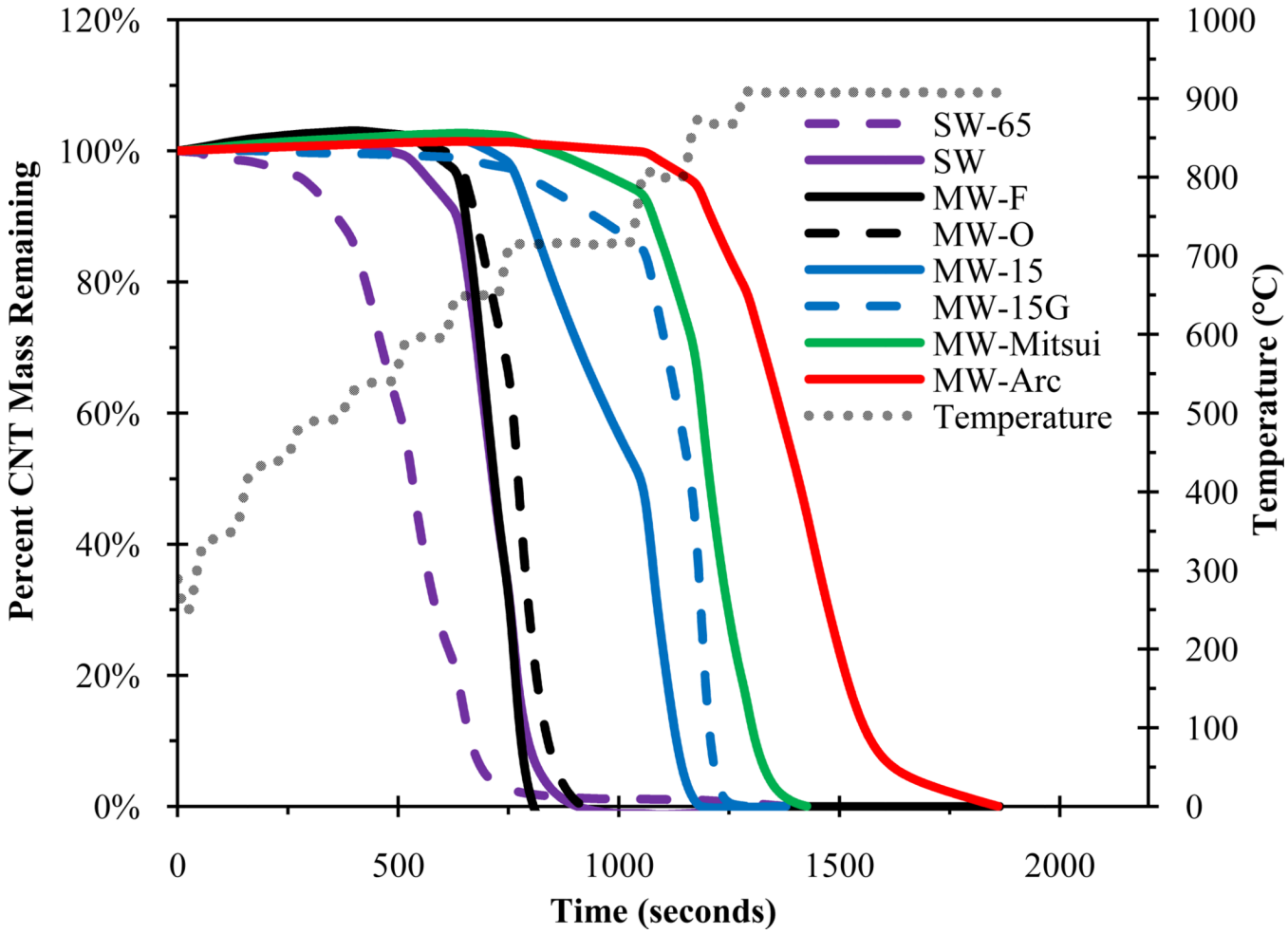

Figure 2.
Percent CNT mass remaining after heating to 910°C under oxidizing conditions. MW-F and MW-O were representative of all other raw CVD MWCNTs not shown.

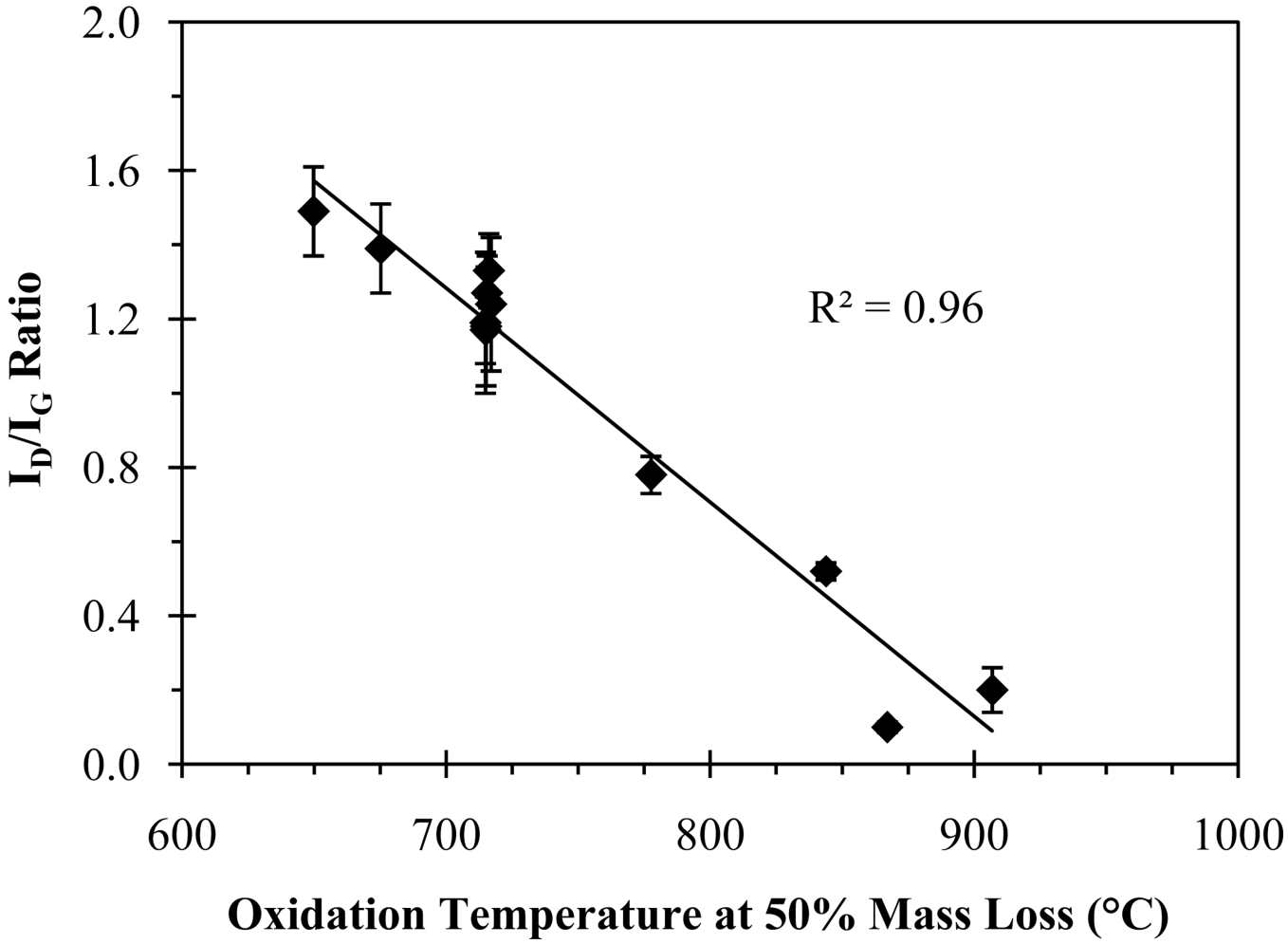

Figure 3.
I_D/I_G ratio as a function of oxidation temperature at 50% mass loss for all MWCNTs.

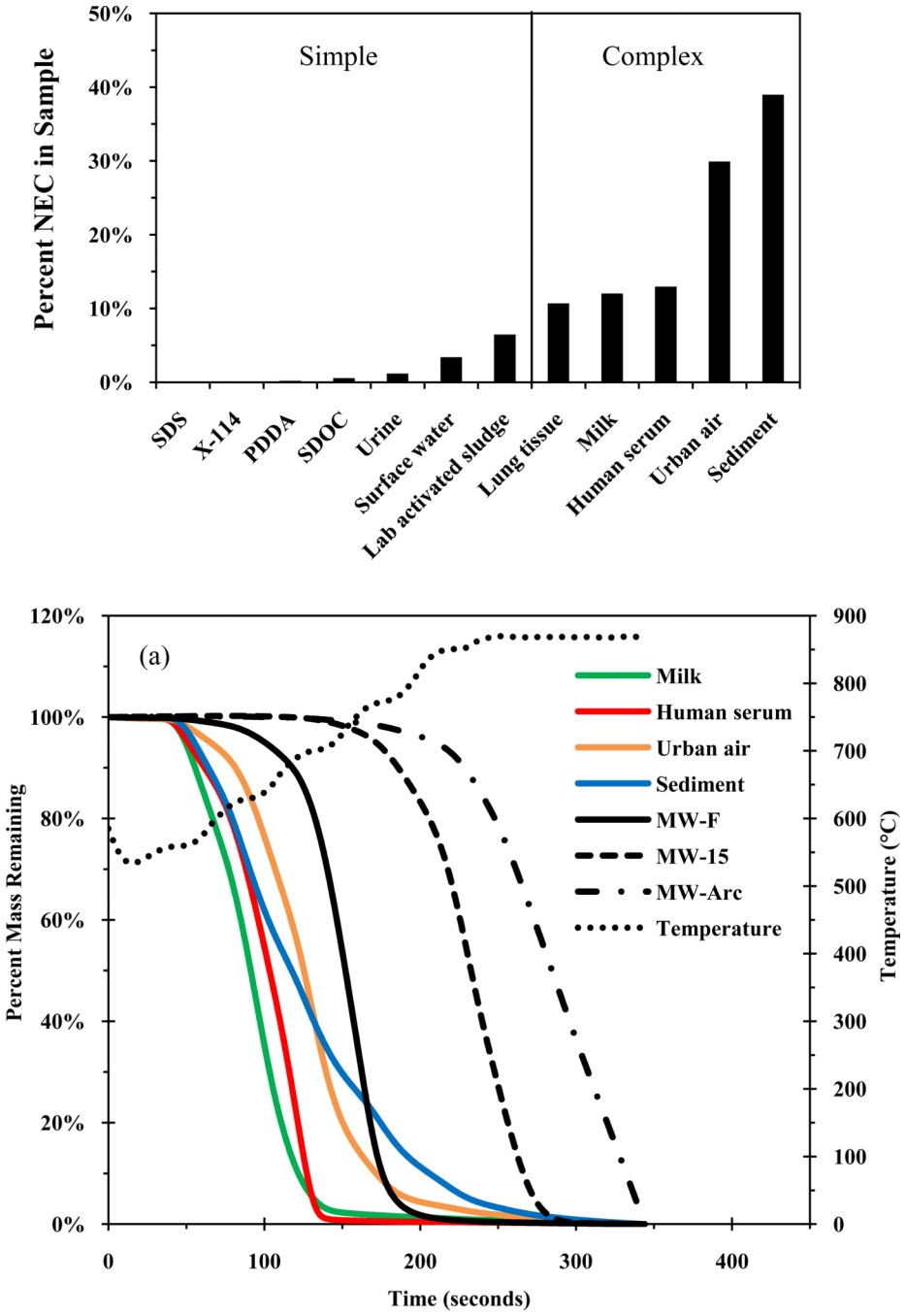

Figure 4.

(a) Percent of NEC (NEC/TC × 100%) present in various laboratory, environmental, and biological matrices. (b) Percent NEC mass remaining from various matrices and percent mass remaining for three CNTs representing the lower (MW-F) and upper (MW-15) range of weak CNTs and strong (MW-Arc) CNTs. NEC mass is the percent remaining after treatment under inert conditions such that all volatile OC has been removed.

Table 1

Properties of CNTs used in this study

CNT ID	CNT Type	State	Purity[a]	Metal Content[b]	Outer Diameter (nm)	Inner Diameter (nm)	Length (μm)
MW-O	MWCNT	Raw	>95%	<6%	20–30	5–10	10–30
MW-P	MWCNT	Purified	>98%	<2%	20–30	5–10	10–30
MW-F	MWCNT	Functionalized	>99.9%	<0.01%	20–30	5–10	10–30
MW-15	MWCNT	Raw	>95%	<5%	7–15	3–6	0.5–200
MW-20	MWCNT	Raw	>95%	<5%	10–20	5–10	0.5–200
MW-30	MWCNT	Raw	>95%	<5%	10–30	5–10	0.5–500
MW-100	MWCNT	Raw	>95%	<5%	60–100	5–10	0.5–500
MW-OH	MWCNT	Functionalized	>95%	<1.5%	8–15	3–5	10–50
MW-COOH	MWCNT	Functionalized	>95%	<1.5%	8–15	3–5	10–50
MW-15G[c]	MWCNT	Annealed	>97%	<1%	7–15	3–6	0.5–200
MW-Mitsui	MWCNT	Raw	>98%	<1%	20–70	NA	NA
MW-Arc	MWCNT[d]	Raw	<50%	0%	5–10[e]	NA	NA
SW	SWCNT	Raw	<50%	<10%	1.1	NA	0.5–100
SW-65	SWCNT	Purified	<75%	<10%	0.8	NA	0.45–2

[a] CNT content reported by manufacturer. MW-P and MW-F calculated assuming no amorphous carbon remaining.

[b] Metal content reported by manufacturer except for MW-F and MW-P determined using energy dispersive X-ray spectroscopy and MW-15G using thermogravimetric analysis.

[c] MW-15 annealed at ~2000°C in UHP He.

[d] Synthesized using arc method; all others are CVD.

[e] Obtained from TEM images; all others reported by manufacturer.